HHS Public Access

Author manuscript

*Gastroenterology*. Author manuscript; available in PMC 2019 April 01.

Published in final edited form as:

*Gastroenterology*. 2018 April ; 154(5): 1480–1493. doi:10.1053/j.gastro.2017.12.004.

# JTC801 Induces pH-dependent Death Specifically in Cancer Cells and Slows Growth of Tumors in Mice

**Xinxin Song**[1,2], **Shan Zhu**[1], **Yangchun Xie**[2], **Jiao Liu**[1], **Lingyi Sun**[3], **Dexing Zeng**[3], **Pengcheng Wang**[4], **Xiaochao Ma**[4], **Guido Kroemer**[5,6,7,8,9,10,11], **David L. Bartlett**[2], **Timothy R. Billiar**[2], **Michael Lotze**[2], **Herbert Zeh**[2], **Rui Kang**[2], and **Daolin Tang**[1,*]

[1]The Third Affiliated Hospital, Center for DAMP Biology, Key Laboratory for Major Obstetric Diseases of Guangdong Province, Key Laboratory of Protein Modification and Degradation of Guangdong Higher Education Institutes, Key Laboratory of Reproduction and Genetics of Guangdong Higher Education Institutes, Guangzhou Medical University, Guangzhou, Guangdong, 510510, China

[2]Department of Surgery, University of Pittsburgh, Pittsburgh, Pennsylvania 15213, USA

[3]Department of Medicine, University of Pittsburgh, Pittsburgh, Pennsylvania 15213, USA

[4]Department of Pharmaceutical Sciences, University of Pittsburgh, Pittsburgh, Pennsylvania 15261, USA

[5]Université Paris Descartes, Sorbonne Paris Cité; 75006 Paris, France

[6]Equipe 11 labellisée Ligue Nationale contre le Cancer, Centre de Recherche des Cordeliers; 75006 Paris, France

[7]Institut National de la Santé et de la Recherche Médicale, U1138; Paris, France

[8]Université Pierre et Marie Curie, 75006 Paris, France

[9]Metabolomics and Cell Biology Platforms, Gustave Roussy Cancer Campus; 94800 Villejuif, France

[10]Pôle de Biologie, Hôpital Européen Georges Pompidou, AP-HP; 75015 Paris, France

[11]Department of Women's and Children's Health, Karolinska University Hospital, 17176 Stockholm, Sweden

## Abstract

[*]Correspondence to: Daolin Tang (tangd2@upmc.edu).



**Disclosure of Potential Conflicts of Interest:** No potential conflicts of interest were disclosed.

**Author Contributions:** D.T. designed the experiments. X.S., S.Z., J.L., Y.X., L.S., D.Z., P.W., X.M., R.K., and D.T conducted the experiments. X.S., G.K., D.L.B., T.R.B., M.T.L, H.J.Z, R.K., and D.T analyzed the data. X.S. and D.T. wrote the paper. G.K., D.L.B., T.R.B., and M.T.L. edited and commented on the manuscript.

**Background & Aims—**Maintenance of acid–base homeostasis is required for normal physiology, metabolism, and development. It is not clear how cell death is activated in response to changes in pH. We performed a screen to identify agents that induce cell death in a pH-dependent manner (we call this alkaliptosis) in pancreatic ductal adenocarcinoma cancer (PDAC) cells and tested their effects in mice.

**Methods—**We screened a library of 254 compounds that interact with G protein-coupled receptors (GPCRs) to identify those with cytotoxic activity against a human PDAC cell line (PANC1). We evaluated the ability of JTC801, which binds the opiod receptor and has analgesic effects, to stimulate cell death in human PDAC cell lines (PANC1, MiaPaCa2, CFPAC1, PANC2.03, BxPc3, and CAPAN2), mouse pancreatic cancer-associated stellate cell lines, primary human pancreatic ductal epithelial cells, and 60 cancer cell lines (the NCI-60 panel). Genes encoding proteins in cell death and GPCR signaling pathways, as well as those that regulate nuclear factor-κB (NF-κB) activity, were knocked out, knocked down, or expressed from transgenes in cancer cell lines. JTC801 was administered by gavage to mice with xenograft tumors, C57BL/6 mice with orthographic pancreatic tumors grown from *Pdx1-Cre;KRas*$^{G12D/+}$;*Tp53*$^{R172H/+}$ (KPC) cells, mice with metastases following tail-vein injection of KPC cells, and *Pdx-1-Cre;Kras*$^{G12D/+}$ mice crossed with *Hmgb1*$^{flox/flox}$ mice (KCH mice). Pancreata were collected from mice and analyzed for tumor growth and by histology and immunohistochemistry. We compared gene and protein expression levels between human pancreatic cancer tissues and patient survival times using online R2 genomic or immunohistochemistry analyses.

**Results—**Exposure of human PDAC cell lines (PANC1 and MiaPaCa2) to JTC801 did not induce molecular markers of apoptosis (cleavage of caspase 3 or poly [ADP ribose] polymerase [PARP]), necroptosis (interaction between receptor-interacting serine-threonine kinase 3 [RIPK3] and mixed lineage kinase domain like pseudokinase [MLKL]), or ferroptosis (degradation of glutathione peroxidase 4 [GPX4]). Inhibitors of apoptosis (Z-VAD-FMK), necroptosis (necrosulfonamide), ferroptosis (ferrostatin-1), or autophagy (hydroxychloroquine) did not prevent JTC801-induced death of PANC1 or MiaPaCa2 cells. The cytotoxic effects of JTC801 in immortalized fibroblast cell lines was not affected by disruption of genes that promote apoptosis (*Bax*$^{-/-}$/*Bak*$^{-/-}$ cells), necroptosis (*Ripk1*$^{-/-}$, *Ripk3*$^{-/-}$, or *Mlkl*$^{-/-}$ cells), ferroptosis (*Gpx4*$^{-/-}$ cells), or autophagy (*Atg3*$^{-/-}$, *Atg5*$^{-/-}$, *Atg7*$^{-/-}$, or *Sqstm1*$^{-/-}$ cells). We found JTC801 to induce a pH-dependent form cell death (alkaliptosis) in cancer cells but not normal cells (hepatocytes, bone marrow CD34$^{+}$ progenitor cells, peripheral blood mononuclear cells, or dermal fibroblasts) or healthy tissues of C57BL/6 mice. JTC801 induced alkaliptosis in cancer cells by activating NF-κB, which repressed expression of the carbonic anhydrase 9 gene (CA9), whose product regulates pH balance in cells. In analyses of Cancer Genome Atlas data and tissue microarrays, we associated increased tumor level of *CA9* mRNA or protein with shorter survival times of patients with pancreatic, kidney, or lung cancers. Knockdown of CA9 reduced the protective effects of NF-κB inhibition on JTC801-induced cell death and intracellular alkalinization in PANC1 and MiaPaCa2 cell lines. Oral administration of JTC801 inhibited growth of xenograft tumors (from PANC1, MiaPaCa2, SK-MEL-28, PC-3, 786-0, SF-295, HCT116, OV-CAR3, and HuH7 cells), orthotropic tumors (from KPC cells), lung metastases (from KPC cells) of mice, and slowed growth of tumors in KCH mice.

**Conclusions—**In a screen of agents that interact with GPCR pathways, we found JTC801 to induce pH-dependent cell death (alkaliptosis) specifically in cancer cells such as PDAC cells, by reducing expression of CA9. Levels of CA9 are increased in human cancer tissues. JTC801 might be developed for treatment of pancreatic cancer.

## Graphical abstract

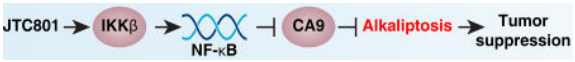


### Keywords

tumor microenvironment; drug development; targeted therapy; pancreas

## Introduction

Cell death comprises two types: accidental cell death and regulated cell death (RCD)[1]. The onset of accidental cell death is extremely fast and doesn't seem to involve any specific molecular machinery. In contrast, the RCD process is tightly controlled by a specific molecular machinery. Apoptosis is a long-recognized type of RCD that eliminates dysfunctional cells under physiological and pathological conditions. However, one hallmark of cancer is the ability of malignant cells to evade apoptosis, which may facilitate tumor development and resistance to traditional therapies[2]. Hence, identification and exploration of non-apoptotic forms of RCD is expected to provide the basis for a rational approach to develop novel targeted therapies.

Aberrant G-protein-coupled receptor (GPCR) expression and activation is implicated in cancer pathogenesis[3]. In this study, we screened compounds in a GPCR library to evaluate their potential anticancer activity. We found that the opioid analgesic compound JTC801 exhibited promising cancer-killing effects not only in pancreatic cancer cell lines, but also in the NCI-60 cell line panel, as well as four different types of mouse pancreatic ductal adenocarcinoma cancer (PDAC) tumor models. Surprisingly, the anticancer activity of JTC801 was not dependent on its known analgesic effect. In contrast, the non-analgesic function of JTC801 contributed to this process via induction of a unique pH-dependent form of RCD that we term alkaliptosis. Surprisingly, induction of alkaliptosis by JTC801 partly required activation of nuclear factor-kappa B (NF-κB), a transcription factor previously shown to promote tumor survival[4]. These unexpected properties reveal new opportunities for pH-dependent cancer therapy by induction of alkaliptosis.

## Materials and Methods

### Antibodies and reagents

The antibodies to CA9, p-RelA, RelA, p-IKKβ, IKKβ, p-IκBα, IκBα, LDH, HIF1α, SQSTM1, cleaved-caspase-3, cleaved-PARP1, NRF2, and actin were obtained from Cell Signaling Technology. The antibodies to GPX4 and CA9 were obtained from Abcam. The antibodies to LC3, MLKL, RIPK3, OPRL1, OPRM1, and HMGB1 were obtained from NOVUS. Desferrioxamine, β-mercaptoethanol, N-acetyl-l-cysteine, N-Acetyl-l-alaine,

hydrogen peroxide solution, gemcitabine hydrochloride, sulfasalazine, cobalt chloride, cycloheximide, tocopherol, necrosulfonamide, hydroxychloroquine sulfate, EDTA, cytochalasin B, cytochalasin D, paclitaxel, crystal violet, protease inhibitor cocktail, Z-VAD-FMK, TNF, staurosporine, cycloheximide, and lipopolysaccharides were obtained from Sigma-Aldrich. Erastin, ferrostatin-1, lapatinib, JTC801, and compound libraries were obtained from Selleck Chemicals. BANORL24, SB612111, UFP101, and Trap101 were obtained from Tocris Bioscience.

## Cell culture

All tumor cell lines were obtained from American Type Culture Collection (ATCC, USA) or the National Cancer Institute (NCI, USA). The mouse PDAC cell line KPC was derived from tumors from KPC mice (*Pdx1-Cre;K-Ras*$^{G12D/+}$ *;p53*$^{R172H/+}$). *Ripk1*$^{-/-}$, *Ripk3*$^{-/-}$, and *Mlkl*$^{-/-}$ mouse embryonic fibroblasts (MEFs) were a gift from Dr. Douglas Green. *Atg5*$^{-/-}$ MEFs were a gift from Dr. Noboru Mizushima. *Atg7*$^{-/-}$ MEFs were a gift from Dr. Masaaki Komatsu. *Sqstm1*$^{-/-}$ MEFs were a gift from Dr. Toru Yanagawa. *Atg3*$^{-/-}$ MEFs were a gift from Dr. Masaaki Komatsu. Inducible *Gpx4*$^{-/-}$ MEFs were a gift from Dr. Marcus Conrad. mPSCs were a gift from Dr. Raul Urrutia. hPDEs were a gift from Dr. Lizhi Cao. *Bax*$^{-/-}$*/Bak*$^{-/-}$ MEFs were purchased from ATCC. Normal human hepatocytes, bone marrow CD34+ progenitor cells, peripheral blood mononuclear cells, and dermal fibroblasts were purchased from Lonza or ATCC. These cells were grown in Dulbecco's Modified Eagle's Medium or RPMI-1640 Medium with 10% fetal bovine serum, 2 mM L-glutamine, and 100 U/ml of penicillin and streptomycin.

## Animal model

We conducted all animal care and experiments in accordance with the Association for Assessment and Accreditation of Laboratory Animal Care guidelines and with approval from the Institutional Animal Care and Use Committee.

To generate murine subcutaneous tumors, 1–5×$10^6$ indicated human cancer cell lines in 100 μl phosphate buffered saline (PBS) were injected subcutaneously to the right of the dorsal midline in female six- to eight-week-old athymic nude mice. Once the tumors reached 50–70 $mm^3$ at day seven, mice were randomly allocated into groups and treated with 10 or 20 mg/kg JTC801 (orally) every day beginning on the seventh day post xenograft injection for two weeks. Tumors were measured twice weekly and volumes were calculated using the formula length×$width^2$×π/6.

To generate orthotopic tumors, C57BL/6 mice were surgically implanted with 5×$10^5$ KPC cells in 10 μl PBS into the pancreas[5]. One week after implantation, mice were randomly allocated into groups and treated with 20 mg/kg JTC801 (orally) every day for three weeks. Animal survival was monitored every week.

To generate metastasis tumors, C57BL/6 mice were injected with 5×$10^5$ KPC in 10 μl PBS into the tail. One week after implantation, mice were randomly allocated into groups and treated with 20 mg/kg JTC801 (orally) every day for two weeks. On day 28, lungs were removed and assayed using histopathology.

*Pdx-1-Cre* and *K-ras*$^{G12D/+}$ transgenic mice on C57BL/6 background were obtained from the Jackson Laboratory. *Hmgb1*$^{flox/flox}$ mice on C57BL/6 background were obtained from Dr. Eugene B. Chang. These mice were crossed to generate indicated KCH animals. At one month of age, mice were randomly allocated into groups and treated with 20 mg/kg JTC801 (orally, twice/week) for four weeks. Animal survival was monitored every week.

***Full Methods*** are available in the SUPPLEMENTAL MATERIALS AND METHODS.

## Results

### JTC801 exhibits selective cytotoxicity

To identify novel PDAC cell-killing agents, we screened a GPCR library of 254 compounds targeting 5-hydroxytryptamine-, dopamine-, opioid-, adrenergic-, cannabinoid-, metabotropic glutamate-, and endothelin-receptors in the human PDAC cell line PANC1. The strongest anticancer activity was observed for JTC801 (Fig. 1A and Table S1). JTC801 also dose-dependently killed five other human PDAC cell lines, mouse pancreatic cancer-associated stellate cell lines (mPSCs), and primary human pancreatic ductal epithelial cells (hPDEs) (Fig. 1B). Colony formation assay further confirmed that JTC801 resulted in a complete long-term growth inhibition in both PDAC and mPSCs (Fig. 1C).

The potency of JTC801 was also independently assessed in a 60-cancer cell line panel (NCI-60) established by the United States National Cancer Institute. The NCI-60 screen revealed increased sensitivity of kidney carcinomas, prostate cancer, melanoma, and central nervous system cancers compared to the other tissues examined (Fig. 1D and S1). We confirmed the potency of JTC801 in these tumor types (Fig. 1E–1G). A rather high dose of JTC801 (100 μM) could interfere with cell viability measurements (Fig. S1). Primary cultures of normal human cells (hepatocytes, bone marrow $CD34^+$ progenitor cells, peripheral blood mononuclear cells, and dermal fibroblasts) were relatively resistant to JTC801 compared to tumor cells (Fig. 1D and 1H). Thus, JTC801 causes growth inhibition and cell death selectively in tumor cells without significantly affecting normal cells.

### JTC801 triggers alkaliptosis

To determine whether the cytotoxicity of JTC801 occurs from the induction of known forms of RCD, we treated cancer cells with JTC801 in the absence or presence of an inhibitor of RCD. The inhibitors of apoptosis (Z-VAD-FMK), necroptosis (necrosulfonamide, “NSA”), ferroptosis (ferrostatin-1), and autophagy (hydroxychloroquine, “HCQ”) failed to block JTC801-induced cell death in PANC1 (Fig. 2A) and MiaPaCa2 cells (Fig. S2A). In contrast, these inhibitors efficiently blocked cell death in response to their corresponding positive stimuli, respectively (Fig. 2A and S2A). Western blot analysis further revealed that JTC801 did not induce molecular events mediating the induction of apoptosis (cleavage of caspase-3 and poly (ADP-ribose) polymerase [PARP]), necroptosis (interaction between receptor-interacting serine-threonine kinase 3 [RIPK3] and mixed lineage kinase domain like pseudokinase [MLKL]), and ferroptosis (glutathione peroxidase 4 [GPX4] degradation) (Fig. 2B–2D and S2B–2D). Moreover, genetic inhibition of apoptosis (*Bax*$^{-/-}$/*Bak*$^{-/-}$ cells) or necroptosis (*Ripk1*$^{-/-}$, *Ripk3*$^{-/-}$, and *Mlkl*$^{-/-}$ cells), as well as removal of a ferroptosis-

related gene (*Gpx4*$^{-/-}$ cells) in immortalized fibroblast cell lines had no influence on JTC801-induced cell killing (Fig. 2F). Despite the fact that JTC801 altered the expression of autophagy-related markers (microtubule associated protein 1 light chain 3 [LC3] and sequestosome 1 [SQSTM1]) (Fig. 2E and S2E), pharmacological inhibition (using HCQ) (Fig. 2A and S2A) or genetic invalidation (*Atg3*$^{-/-}$, *Atg5*$^{-/-}$, *Atg7*$^{-/-}$, and *Sqstm1*$^{-/-}$ cells) (Fig. 2F) of autophagy failed to affect the cytotoxicity of JTC801. JTC801 induced a necrosis-like morphology (Fig. S3A) and propidium iodide positivity (Fig. S3B). Consistently, JTC801 triggered the cellular release of membrane damage markers such as lactate dehydrogenase (LDH) and high mobility group box 1 (HMGB1) (Fig. S3C). Thus, JTC801-induced cell death appears to be a form of regulated necrosis.

We next tested whether ion channel ligands would affect JTC801 activity. Pharmacological compounds targeting calcium channels (cilnidipine, ranolazine, and isradipine), potassium channels (repaglinide, nicorandil, and amiodarone), and sodium channels (oxcarbazepine, riluzole, and carbamazepine) had no measurable effect on JTC801 potency (Fig. 2G). Other drugs interfering with cell death such as cytoskeleton-targeting drugs (taxol, cytochalasin B or D) and metal chelators (ethylenediaminetetraacetic acid [EDTA] and desferrioxamine [DFO]) also failed to affect JTC801 activity (Fig. 2G).

In contrast, N-acetyl cysteine (NAC), a synthetic precursor of the endogenous cellular antioxidant glutathione (GSH) with broad cytoprotective effects, remarkably diminished JTC801-induced cell death (Fig. 2G and 2H). Intriguingly, the levels of GSH (Fig. S4A) and CM-H2DCFDA (a general oxidative stress indicator, Fig. S4B) were not affected by JTC801 compared to other RCD stimuli (ferroptosis-inducing erastin and pro-apoptotic staurosporine). We therefore hypothesized that NAC may play an antioxidant-independent role in mediating the protection against JTC801-induced cell death. Consistent with this hypothesis, other antioxidants (β-mercaptoethanol [β-ME] and vitamin E) (Fig. 2G) did not ameliorate JTC801-induced cell death. Moreover, knockdown of nuclear factor (erythroid-derived 2)-like 2 (NRF2), a transcription factor for antioxidant enzymes, did not alter JTC801-induced cell death (Fig. S4C and S4D).

As a weak acid, NAC alters extracellular pH to 6.11 when prepared at work concentrations in the cell medium[6]. To determine whether the NAC-mediated acidic pH environment limits JTC801-induced cell death, we treated PANC1 cells with N-acetyl alanine acid (NAA), a compound structurally similar to NAC that conserves acid activity but loses all antioxidant activity[7]. Glutathione disulfide (GSSG) is a disulfide derived from two GSH molecules. NAC, but not JTC801 and NAA, increased the GSH/GSSG ratio (Fig. S5A). Like NAC, NAA rescued cells from JTC801-induced death (Fig. 2G, 2H, and S5B). Adjusting the extracellular pH with HCl from a normal pH of 7.21 to an acidic pH of 6.2 also prevented JTC801-induced cell death (Fig. 2H and S5B). In contrast, alkalinization of the cell culture medium with sodium hydroxide diminished the protective activity of NAC on JTC801-induced cell death (Fig. 2H and S5B). Pre-exposure of JTC801 to an acidic pH (pH 2–6) did not alter its cytotoxic activity (Fig. S6A and S6B), contradicting the possibility that protonation would affect the drug itself.

Next, we determined whether JTC801 directly influences extracellular and intracellular pH to trigger death. Surprisingly, intracellular pH (Fig. 2I and S5C), but not extracellular pH (Fig. 2J and S5D) was shifted toward basic values in response to JTC801. This intracellular alkalinization was inhibited by NAC, NAA, and acidic medium (pH 6.2) (Fig. 2I and S5C). Unlike JTC801, other RCD stimuli (pro-apoptotic staurosporine, pro-necroptotic tumor necrosis factor [TNF], and ferroptosis-inducing erastin) did not provoke intracellular alkalinization (Fig. S6C and S6D). Collectively, these data suggest that JTC801 triggers an intracellular alkalinization-dependent form of regulated necrosis that we termed 'alkaliptosis' (Fig. 2K).

## OPRL1 is not required for alkaliptosis

JTC801 was originally identified as a selective antagonist for OPRL1 with analgesic activity[8]. To understand more precisely how JTC801 causes cell death, we used five different approaches to assess whether the sensitivity to alkaliptosis is dependent on the expression of OPRL1. First, several cancer cells (CFPAC1, PANC2.03, BxPc3, CAPAN2, and HCT116) with low protein expression of OPRL1 were still sensitive to JTC801-induced alkaliptosis (Fig. 3A and 3B). Second, knockdown of OPRL1 by shRNA in cells with a high expression of OPRL1 (PANC1 and MiaPaCa2) did not suppress JTC801-induced alkaliptosis (Fig. 3C and 3D). Third, unlike JTC801, other OPRL1 antagonists (BANORL24, SB612111, UFP101, and Trap101) did not trigger cell death (Fig. 3E). Fourth, two analogues of JTC801 with higher (A1) or lower (A2) binding affinity for OPRL1 displayed similar anticancer activity (Fig. 3F and 3G). In contrast, three other JTC801 analogues (A3–A5) that were characterized by a modified amine group at position 4 of the quinoline, released amine group at position 6 of the quinoline, and the removal of the phenoxymethyl group lost their cytotoxicity (Fig. 3F and 3G). Modifying substituents on the phenoxymethyl group of JTC801 (A6–A7) partially abrogated its cytotoxicity (Fig. 3F and 3G). Fifth, knockdown of other opioid receptors such as OPRM1 failed to block JTC801-induced cell death (Fig. 3H and 3I). Together, these findings suggest that the expression of OPRL1 or OPRM1 may not be essential for JTC801-induced alkaliptosis.

## NF-κB contributes to alkaliptosis

To identify key players in the modulation of alkaliptosis, we treated PANC1 cells with JTC801 in the absence or presence of a panel of 416 kinase or protease inhibitors. IMD0354, a selective inhibitor of I-kappa-B-kinase (IKK) beta (IKKβ), was most active in reducing the cytotoxic activity of JTC801 (Fig. 4A and Table S2). IMD0354 not only inhibited cell death (Fig. 4B and S7A), but also prevented the intracellular alkalinization induced by JTC801 (Fig. 4C and S7B). Other IKKβ inhibitors (CAY10657 and SC514) also increased cell survival (Fig. 4B and S7A) and decreased intracellular pH (Fig. 4C and S7B) in response to JTC801. The extracellular pH was not affected by IKKβ inhibitors (Fig. 4D and S7C).

IKKβ is a kinase of the IKK enzyme complex. Activation of the transcription factor NF-κB mainly occurs via IKK-mediated phosphorylation of inhibitory molecules, including I-kappa-B alpha (IκBα). This phosphorylation serves as a signal for subsequent ubiquitination, which promotes IκBα degradation and the release of NF-κB from its inhibition, allowing its translocation from the cytoplasm to the nucleus. JTC801 triggered

the phosphorylation of IKKβ and IκBα, as well as the subsequent degradation of IκBα (Fig. 4E and S7D). Optimal induction of NF-κB target genes requires phosphorylation of NF-κB proteins such as RelA/p65. JTC801 also induced RelA phosphorylation (Fig. 4E and S7D). These changes indicate that alkaliptosis occurs in the context of the activation of the NF-κB.

Next, we silenced the gene expression of IKKβ or RelA, each with two different shRNAs, in PANC1 (Fig. 4F) and MiaPaCa2 cells (Fig. S7E). In both settings, we found that suppression of IKKβ or RelA expression partly prevented JTC801-induced cell death (Fig. 4G and S7F) and intracellular alkalinization (Fig. 4H and S7G). Extracellular pH was not significantly affected by the knockdown of IKKβ or RelA (Fig. 4I and S7H). Knockdown of IKKβ or RelA increased staurosporine-induced cell death in PANC1 (Fig. 4J) and MiaPaCa2 (Fig. S7I) cells, consistent with previous reports that the NF-κB plays a pro-survival role in the regulation of apoptosis[9]. Together, these results uncover an unexpected role for the NF-κB in mediating alkaliptosis.

## CA9 downregulation contributes to alkaliptosis

Cancer cells reportedly maintain intracellular pH via changes in the expression or activity of several molecules such as carbonic anhydrase (“CA”, CA2, CA9, and CA12), monocarboxylate transporter (“MCT”, MCT1, MCT2, MCT3, and MCT4), vacuolar ATPase pumps (“V-ATPase”, V-ATPaseA and V-ATPaseB), $Na^+$-dependent $Cl^-$-$HCO3^-$ exchanger (NDCBE), $Na^+$-coupled $HCO3^-$ transporter (“NBC”, NBC1/2), anion exchanger (“AE”, AE1, AE2, and AE3), and $Na^+$-$H^+$ exchanger 1 (NHE1) (Fig. 5A)[10]. The mRNA expression of CA9 and NDCBE were suppressed in both PANC1 and MiaPaCa2 cells under JTC801-induced alkaliptosis (Fig. 5B). Pharmacological or genetic blockage of the NF-κB activity reversed JTC801-induced downregulation of CA9 (but not NDCBE) mRNA (Fig. 5C, 5D, and S8A). Western blot analysis confirmed that JTC801 suppressed CA9 protein expression and that this process was prevented by blocking the NF-κB activity (Fig. 5E and S8B). These findings, in combination with further luciferase reporter-gene activation assays (Fig. 5F and S8C), indicate that CA9 is a negative target of NF-κB in alkaliptosis.

We next determined whether other NF-κB stimuli such as bacterial lipopolysaccharides (LPS) had effects similar to that of JTC801 on alkaliptosis. LPS did not induce intracellular alkalinization (Fig. 5G) and CA9 downregulation (Fig. 5H) in PANC1 cells, indicating that other mechanisms play a role in the regulation of JTC801-induced CA9 downregulation in alkaliptosis. Indeed, the cycloheximide chase assay showed that JTC801 promoted CA9 protein degradation (Fig. 5I), suggesting that CA9 expression is regulated by both transcriptional and post-transcriptional mechanisms in alkaliptosis.

Given that hypoxia inducible factor 1 alpha subunit (HIF1α) also controls CA9 gene expression in hypoxia, we next verified whether HIF1α is involved in the regulation of CA9 expression in alkaliptosis. The protein levels of HIF1α and CA9 were increased in response to $CoCl_2$ (a chemical inducer of HIF1α) (Fig. S9). However, HIF1α expression was not affected by JTC801 in alkaliptosis (Fig. S9). $CoCl_2$ did not prevent JTC801-induced CA9 downregulation (Fig. S9). These findings indicate that HIF1α may not be required for CA9 expression in alkaliptosis.

Survival analysis of patients in The Cancer Genome Atlas (TCGA), integrating gene expression data, indicated that CA9 mRNA expression is associated with shorter survival times of patients with pancreatic, kidney, or lung cancers (Fig. 6A). Immunohistochemical analysis of a tissue microarray comprising samples from 90 pancreatic cancer patients confirmed that high CA9 expression (Fig. 6B) is associated with shorter survival times (Fig. 6C). These results provide correlative clinical evidence that high expression of CA9 gene or protein is associated with the progression of multiple types of cancer, including pancreatic cancer.

We next sought to define the mechanism of action of CA9 in alkaliptosis. Overexpression of CA9 by gene transfection reduced JTC801-induced cell death (Fig. 6D, 6E, S10A, and S10B). In contrast, genetic suppression of CA9 enhanced JTC801-induced cell death (Fig. 6F, 6G, S10C, and S10D). Consistently, JTC801-induced intracellular pH upregulation was decreased by CA9 overexpression, confirming that CA9 modulates intracellular alkalinization in alkaliptosis (Fig. 6H and S10E). As expected, CA9 did not affect extracellular pH in response to JTC801 (Fig. 6I and S10F). Knockdown of CA9 attenuated the protective effects of NF-κB inhibition on JTC801-induced cell death and intracellular alkalinization (Fig. 6J–L and S10G–I). Knockdown of CA9 did not significantly affect intracellular pH at baseline (Fig. 6H and S10E), indicating that CA9-mediated acid-base homeostasis is stress dependent and changes in alkaliptosis.

## Anticancer activity of JTC801 in vivo

Driven by the consideration that JTC801 was stable in acidic environments (pH 2–6) *in vitro* (Fig. S6A and S6B), we tested the oral pharmacokinetics of JTC801 *in vivo*. We found that peak plasma concentration was achieved at one to four hours after administration of JTC801 by gavage to C57BL/6 mice (Fig. S11A). The plasma half-life of JTC801 was 8.2 hours. Like most drugs, JTC801 quickly accumulated in the liver and then in the kidney (Fig. S11B). Interestingly, a considerable amount of JTC801 was detectable in the pancreas (Fig. S11B). Oral administration of JTC801 at 20 mg/kg for one week to mice did not lead to weight loss (Fig. S12A), abnormal behavior, or histological signs of tissues injury (Fig. S12B). JTC801 also failed to induce biochemical signs of toxicity such as elevated plasma concentrations of alanine aminotransferase [ALT], blood urea nitrogen [BUN], and amylase [AMYL] (Fig. S12C). These findings are consistent with those from another study showing that oral administration of JTC801 at 30 mg/kg is safe in rats[11].

Next, we investigated the potential utility of alkaliptosis for cancer suppression *in vivo* in four distinct preclinical mouse models. Oral administration of JTC801 alone remarkably blocked PANC1 tumor growth in a nude mouse xenograft model (Fig. 7A–C) with decreased CA9 expression and increased RelA phosphorylation in the tumor (Fig. 7D). This anticancer activity of JTC801 was also observed in mouse xenograft models of human cancer cell lines including MiaPaCa2 (a human pancreatic cancer cell line), SK-MEL-28 (a human melanoma cell line), PC-3 (a human prostate cancer cell line), 786-0 (a human kidney cancer cell line), SF-295 (a brain cancer cell line), HCT116 (a human colon cancer cell line), OV-CAR3 (a human ovarian cancer cell line), and HuH7 (a human liver cancer cell line) (Fig. S13A). Accordingly, the mRNA levels of CA9 were decreased in these tumors after administration

of JTC801 (Fig. 7E and S13B). Liver and kidney function did not change in the nude mouse xenograft models after administration of JTC801 (Fig. S13C).

We further observed that administration with JTC801 prolonged the survival of C57BL/6 mice after orthotropic implantation of KPC cells into the pancreas by surgery (Fig. 7F). Accordingly, tumor size (Fig. 7G) and weight (Fig. 7H) were reduced after administration of JTC801. JTC801 was also effective in preventing lung metastasis induced by tail vein injection of KPC cells (Fig. 7I–K), supporting the anti-metastatic activity of JTC801 *in vivo*.

We recently developed a genetically engineered mouse model of accelerated PDAC by combining original *K-Ras*$^{G12D/+}$-driven PDAC models with additional loss of the chromatin protein HMGB1 in pancreatic tissue (*Pdx1-Cre;K-Ras*$^{G12D/+}$*;HMGB1*$^{-/-}$, termed KCH mice)[12]. JTC801 prolonged the survival of KCH animals (Fig. 7L), as it reduced pancreatic ductal lesion formation and desmoplastic stromal responses (Fig. 7M and 7N). CA9 was downregulated, whereas RelA phosphorylation (Fig. 7O and 7P) was increased in tumors from KCH mice in response to JTC801. Collectively, these preclinical results demonstrated that JTC801 possesses potent anti-tumor activity *in vivo*.

## Discussion

An unbalanced pH level can lead to different types of cell death. Intracellular acidification was previously identified to be involved in apoptosis[13], necroptosis[14], and autophagy[15]. In contrast, little is known about the role of intracellular alkalinization in RCD, although alkalosis is associated with various pathological conditions. Here, we demonstrate that, in cancer cells, JTC801-induced intracellular alkalinization triggers a novel modality of RCD termed alkaliptosis. These findings shed new light on the understanding of the fundamental process of pH homeostasis in RCD.

Alkaliptosis is biochemically and genetically distinct from various forms of RCD. Signs of caspase activation, necrosome assembly, or lipid peroxidation were not observed in alkaliptosis. Genetic and pharmacological inhibition of apoptosis, necroptosis, autophagy, and ferroptosis was unable to block JTC801-induced alkaliptosis. In contrast, alkaliptosis apparently constitutes a regulated form of necrosis based on the fact that it shares many morphological features with primary necrosis, as well as the release of endogenous damage-associated molecular patterns. Unlike other forms of RCD, oxidative stress and activation of ion channels were not essential for JTC801-induced alkaliptosis. Rather, this process is characterized by intracellular alkalinization, which, at the molecular level, is partly induced by the NF-κB activity.

The NF-κB pathway is generally considered as a prosurvival signaling pathway that acts in conditions of inflammation[16]. Thus NF-κB transactivates a series of proinflammatory and anti-apoptotic genes. In the current study, activation of NF-κB promoted alkaliptosis depending on the inhibition of CA9, a member of the carbonic anhydrase family. Knockdown of CA9 not only recapitulated the activation of the NF-κB pathway-mediated intracellular alkalinization phenotype, but also restored alkaliptosis sensitivity in cells with low NF-κB activity. Thus, potential upstream regulators and downstream targets can

determine stimulus-dependent activation of NF-κB in promoting either cell survival or cell death[17]. JCT801 displayed selective toxicity for cancer cells, but not normal cells. One possible mechanism accounting for this difference is that the expression level of pH regulation molecules such as CA9 differs between cancer and normal cells[18].

Pharmacological or genetic inhibition of the NF-κB activity partly reversed alkaliptosis, indicating that other pathways such as the selective protein degradation pathway are involved in the regulation of intracellular alkalinization. Knowledge of acid-base homeostasis in normal and cancer cells and information about gene expression patterns under alkaliptosis all have the potential to provide insights into interpreting the phenotype and direction for further investigation, especially when considered in targeted cancer therapies.

The current studies summarize preclinical evidence suggesting that JCT801 might be useful for the treatment of human cancers, especially PDAC. One of the reasons for this low survival rate of PDAC is the insensitivity of pancreatic cancer to most chemotherapies, as well as the scarce distribution of drugs into the pancreas. Our studies document that oral administration of JTC801 resulted in a distribution of the drug towards the pancreas. JTC801 inhibited tumor growth in four different PDAC mouse models without any significant toxicity. In addition to its cytotoxic activity across a panel of multiple tumor cell type, another potential advantage of JTC801 may reside in its analgesic function. Thus, JTC801 may be especially useful for cancer patients with pain and anxiety symptoms. The anticancer and analgesic actions of JCT801 can be dissociated at the structural level. Indeed, OPRL1 is not required for JTC801-induced alkaliptosis. Further investigations are needed to identify the molecular target responsible for the anticancer activity of JTC801.

## Supplementary Material

Refer to Web version on PubMed Central for supplementary material.

## Acknowledgments

We thank Christine Heiner (Department of Surgery, University of Pittsburgh) for her critical reading of the manuscript.

**Grant Support:** This work was supported by grants from the US National Institutes of Health (R01GM115366, R01CA160417, R01CA181450, and R01CA211070), the Natural Science Foundation of Guangdong Province (2016A030308011), the American Cancer Society (Research Scholar Grant RSG-16-014-01-CDD), the National Natural Science Foundation of China (31671435, 81400132, and 81772508), and Guangdong Province Universities and Colleges Pearl River Scholar Funded Scheme (2017). This project partly utilized University of Pittsburgh Cancer Institute shared resources supported by award P30CA047904. G.K. is supported by the Ligue contre le Cancer (équipe labelisée); Agence National de la Recherche (ANR) – Projets blancs; ANR under the frame of E-Rare-2, the ERA-Net for Research on Rare Diseases; Association pour la recherche sur le cancer (ARC); Cancéropôle Ile-de-France; Institut National du Cancer (INCa); Institut Universitaire de France; Fondation pour la Recherche Médicale (FRM); the European Commission (ArtForce); the European Research Council (ERC); the LeDucq Foundation; the LabEx Immuno-Oncology; the RHU Torino Lumière, the SIRIC Stratified Oncology Cell DNA Repair and Tumor Immune Elimination (SOCRATE); the SIRIC Cancer Research and Personalized Medicine (CARPEM); and the Paris Alliance of Cancer Research Institutes (PACRI).

## References


1. Galluzzi L, Bravo-San Pedro JM, Vitale I, et al. Essential versus accessory aspects of cell death: recommendations of the NCCD 2015. Cell Death Differ. 2014
2. Hanahan D, Weinberg RA. Hallmarks of cancer: the next generation. Cell. 2011; 144:646–74. [PubMed: 21376230]
3. O'Hayre M, Vazquez-Prado J, Kufareva I, et al. The emerging mutational landscape of G proteins and G-protein-coupled receptors in cancer. Nat Rev Cancer. 2013; 13:412–24. [PubMed: 23640210]
4. Pikarsky E, Porat RM, Stein I, et al. NF-kappaB functions as a tumour promoter in inflammation-associated cancer. Nature. 2004; 431:461–6. [PubMed: 15329734]
5. Xie Y, Zhu S, Zhong M, et al. Inhibition of Aurora Kinase A Induces Necroptosis in Pancreatic Carcinoma. Gastroenterology. 2017; 153:1429–1443. e5. [PubMed: 28764929]
6. Noszal B, Visky D, Kraszni M. Population, acid-base, and redox properties of N-acetylcysteine conformers. J Med Chem. 2000; 43:2176–82. [PubMed: 10841796]
7. Platzer G, Okon M, McIntosh LP. pH-dependent random coil (1)H, (13)C, and (15)N chemical shifts of the ionizable amino acids: a guide for protein pK a measurements. J Biomol NMR. 2014; 60:109–29. [PubMed: 25239571]
8. Yamada H, Nakamoto H, Suzuki Y, et al. Pharmacological profiles of a novel opioid receptor-like1 (ORL(1)) receptor antagonist, JTC-801. Br J Pharmacol. 2002; 135:323–32. [PubMed: 11815367]
9. Millan O, Ballester A, Castrillo A, et al. H-Ras-specific activation of NF-kappaB protects NIH 3T3 cells against stimulus-dependent apoptosis. Oncogene. 2003; 22:477–83. [PubMed: 12555061]
10. Webb BA, Chimenti M, Jacobson MP, et al. Dysregulated pH: a perfect storm for cancer progression. Nat Rev Cancer. 2011; 11:671–7. [PubMed: 21833026]
11. Tamai H, Sawamura S, Takeda K, et al. Anti-allodynic and anti-hyperalgesic effects of nociceptin receptor antagonist, JTC-801, in rats after spinal nerve injury and inflammation. Eur J Pharmacol. 2005; 510:223–8. [PubMed: 15763246]
12. Kang R, Xie Y, Zhang Q, et al. Intracellular HMGB1 as a novel tumor suppressor of pancreatic cancer. Cell Res. 2017; 27:916–932. [PubMed: 28374746]
13. Furlong IJ, Ascaso R, Lopez Rivas A, et al. Intracellular acidification induces apoptosis by stimulating ICE-like protease activity. J Cell Sci. 1997; 110(Pt 5):653–61. [PubMed: 9092947]
14. Wang YZ, Wang JJ, Huang Y, et al. Tissue acidosis induces neuronal necroptosis via ASIC1a channel independent of its ionic conduction. Elife. 2015; 4
15. Nakamura N, Matsuura A, Wada Y, et al. Acidification of vacuoles is required for autophagic degradation in the yeast, Saccharomyces cerevisiae. J Biochem. 1997; 121:338–44. [PubMed: 9089409]
16. Lawrence T. The nuclear factor NF-kappaB pathway in inflammation. Cold Spring Harb Perspect Biol. 2009; 1:a001651. [PubMed: 20457564]
17. Hayden MS, Ghosh S. NF-kappaB, the first quarter-century: remarkable progress and outstanding questions. Genes Dev. 2012; 26:203–34. [PubMed: 22302935]
18. Benej M, Pastorekova S, Pastorek J. Carbonic anhydrase IX: regulation and role in cancer. Subcell Biochem. 2014; 75:199–219. [PubMed: 24146381]

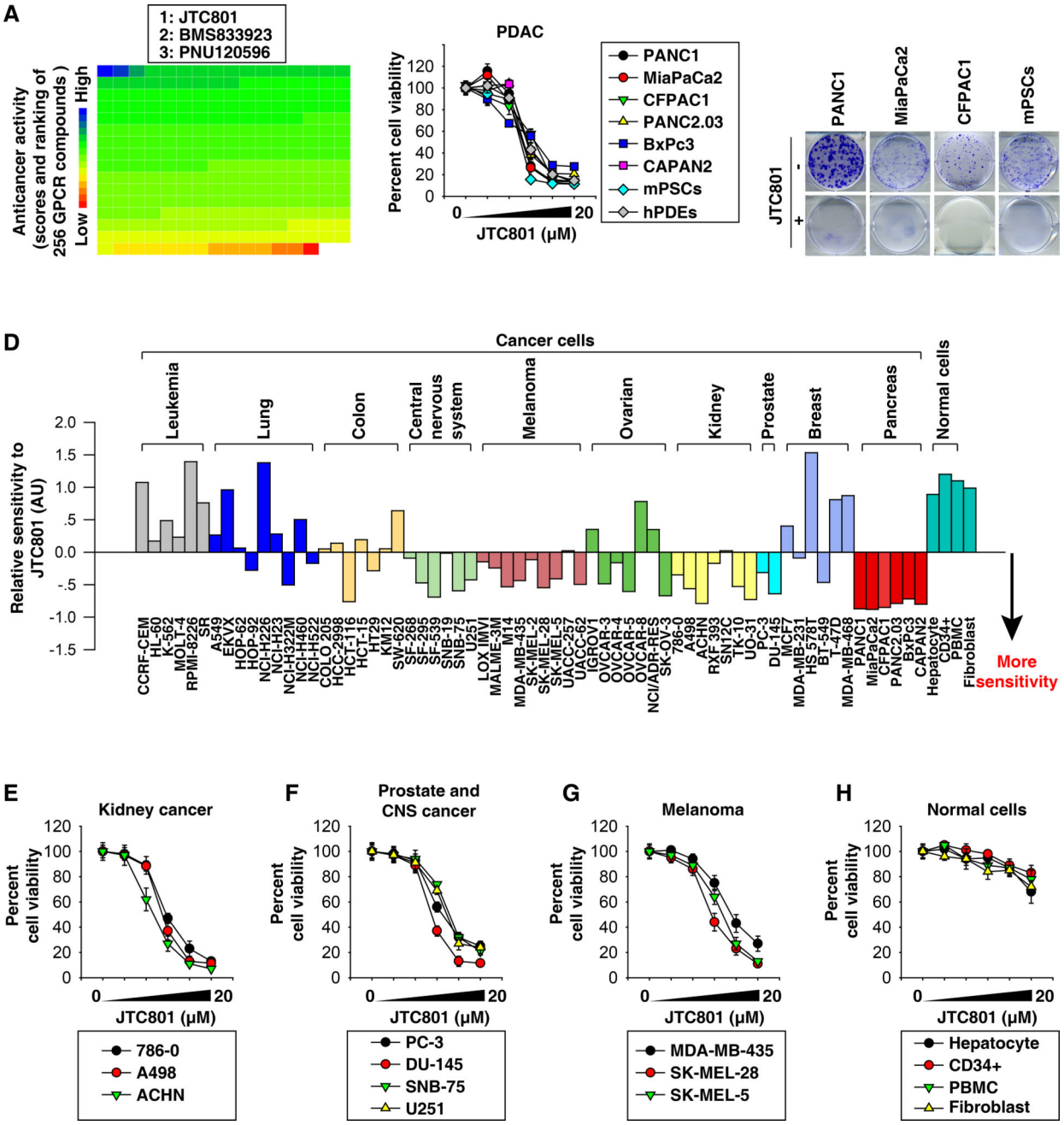


**Fig. 1. Anticancer activity of JTC801 *in vitro***

(A) PANC1 cells were treated with a GPCR compound (10 μM) for 24 hours and then cell viability was assayed. The ranking of the relative anticancer activity of 254 GPCR compounds is shown by the heat map; each block represents one GPCR compound. The top three anti-cancer GPCR compounds are listed. (B) Indicated human PDAC cell lines, mPSCs, and hPDEs were treated with JTC801 (1.25–20 μM) for 24 hours. Cell viability was assayed (n=3). (C) Clonogenic cell survival assay determined the reproductive ability of a cell in response to JTC801 (10 μM). (D) Sensitivity profile of 66 cancer cell lines and four normal cell types against JTC801. The cells were grouped based on their tissue origins. (E–

H) Indicated cancer or normal cells were treated with JTC801 (1.25–20 μM) for 24 hours. Cell viability was assayed (n=3).

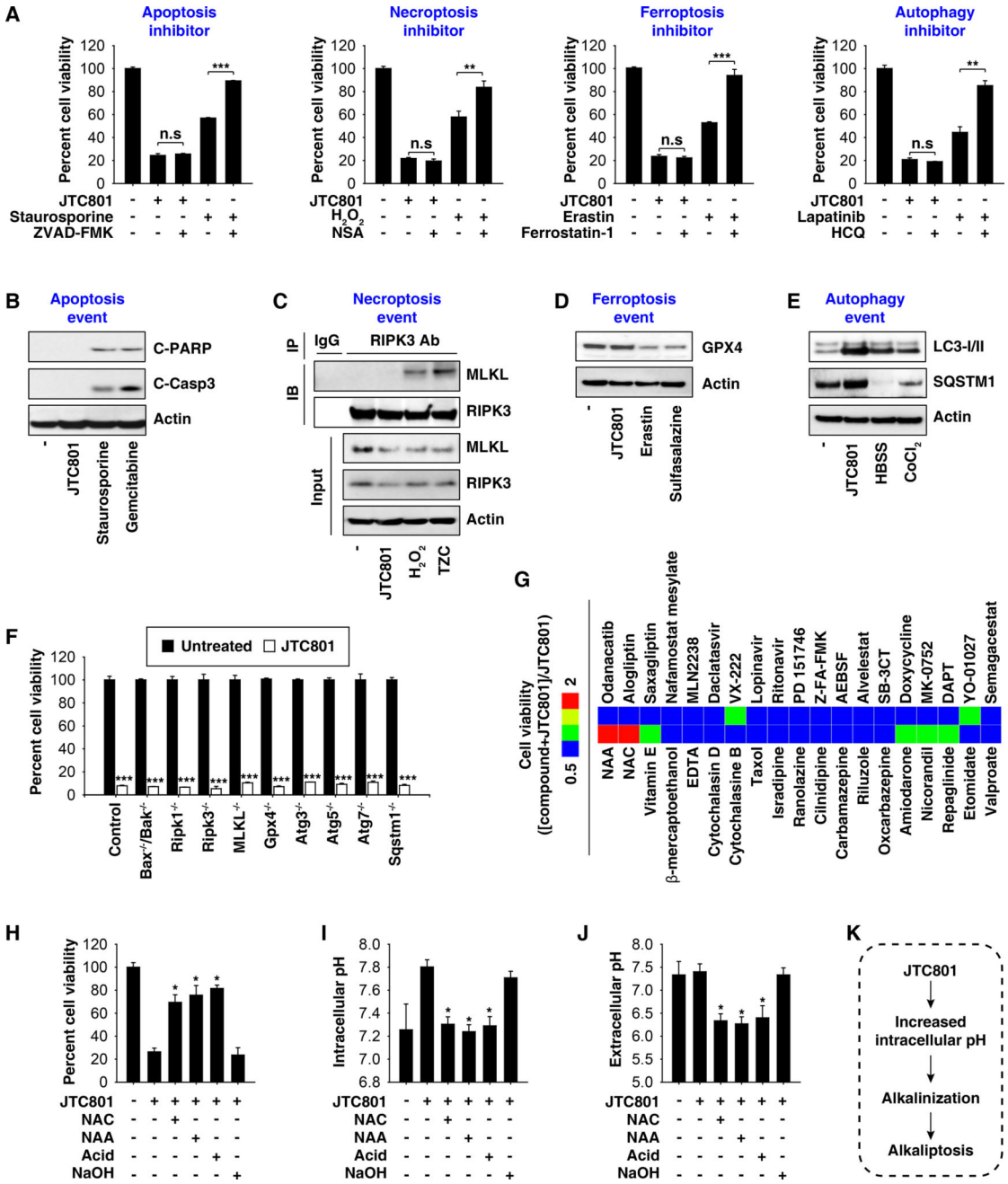


**Fig. 2. JTC801 induces alkaliptosis**

(A) PANC1 cells were treated with JTC801 (10 μM), staurosporine (0.5 μM), erastin (20 μM), $H_2O_2$ (500 μM), or lapatinib (50 μM) in the absence or presence of ZVAD-FMK (20 μM), ferrostatin-1 (500 nM), necrosulfonamide ("NSA", 1 μM), and hydroxychloroquine ("HCQ", 50 μM) for 24 hours. Cell viability was assayed (n=3, **p < 0.01, ***p < 0.001, n.s.=not significant). (B) PANC1 cells were treated with JTC801 (10 μM), staurosporine (1 μM), or gemcitabine (5 mM) for 24 hours and the levels of cleaved-PARP ("C-PARP"), cleaved-caspase 3 ("C-Casp3"), and actin were assayed using western blot. (C) PANC1 cells were treated with JTC801 (10 μM), $H_2O_2$ (500 μM), or TZC (TNF [50 nM]/ZVAD-FMK

[20 μM]/cycloheximide [10 μg/ml]) for 24 hours. Cell lysates were immunoprecipitated with anti-RIPK3 antibody or control IgG, and then the levels of MLKL and RIPK3 were assayed using western blot. (D) PANC1 cells were treated with JTC801 (10 μM), erastin (20 μM), or salazosulfapyridine (1 mM) for 24 hours and then the levels of GPX4 and actin were assayed using western blot. (E) PANC1 cells were treated with JTC801 (10 μM, 24 hours), $CoCl_2$ (400 μM, 24 hours), or Hank's buffered salt solution (HBSS, 6 hours), and the levels of LC3-I/-II, SQSTM1, and actin were assayed using western blot. (F) Indicated gene-deficient cells were treated with JTC801 (10 μM) for 24 hours, and then cell viability was assayed (n=3, ***$p < 0.001$ versus untreated group). (G) PANC1 cells were treated with JTC801 (10 μM) in the absence or presence of the indicated compounds (10 μM) for 24 hours, and then cell viability was assayed. The ratio in the heat map was defined as cell viability ([Compound +JTC801]/JTC801). (H–J) PANC1 cells were treated with JTC801 (10 μM) in the absence or presence of N-acetylcysteine (“NAC”, 100 mM), N-acetyl alanine acid (“NAA”, 100 mM), acidic medium (pH=6, adjusted by HCl), and NAC (100 mM, pH=7, adjusted by NaOH) for 24 hours. Cell viability, intracellular pH, and extracellular pH were assayed (n=3, *$p < 0.05$ versus JTC801 group). (K) Schematic depicting JTC801-induced alkaliptosis.

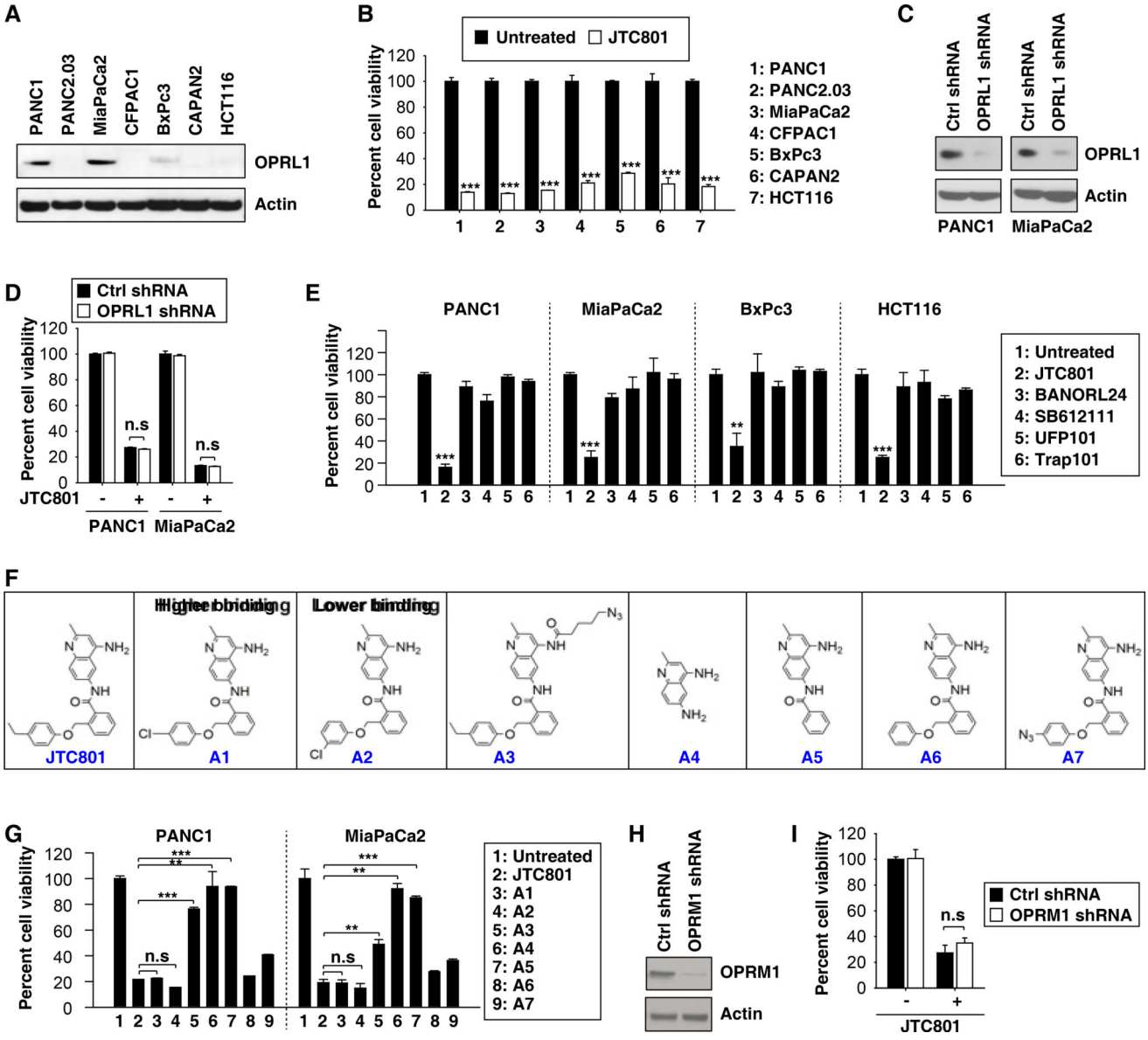


**Fig. 3. OPRL1 is not required for JTC801-induced alkaliptosis**

(A) Western blot analysis of OPRL1 expression in cancer cells. (B) Cancer cells were treated with JTC801 (10 μM) for 24 hours and then cell viability was assayed (n=3, ***p < 0.001 versus untreated group). (C) Western blot analysis of OPRL1 expression in OPRL1-knockdown PANC1 and MiaPaCa2 cells. (D) Knockdown of OPRL1 did not affect JTC801 (10 μM, 24 hours)-induced cell death in PANC1 and MiaPaCa2 cells (n=3, n.s=not significant). (E) Cancer cells were treated with JTC801 or indicated OPRL1 antagonists at 10 μM for 24 hours. Cell viability was assayed (n=3, **p < 0.01, ***p < 0.001 versus untreated group). (F) Structure of JTC801 and its analogues. (G) PANC1 and MiaPaCa2 cells were treated with JTC801 and its analogues at 10 μM for 24 hours. Cell viability was assayed (n=3, **p < 0.01, ***p < 0.001, n.s=not significant). (H) Western blot analysis of OPRM1 expression in OPRL1-knockdown PANC1 cells. (I) Knockdown of OPRM1 did not

affect JTC801 (10 μM, 24 hours)-induced cell death in PANC1 cells (n=3, n.s=not significant).

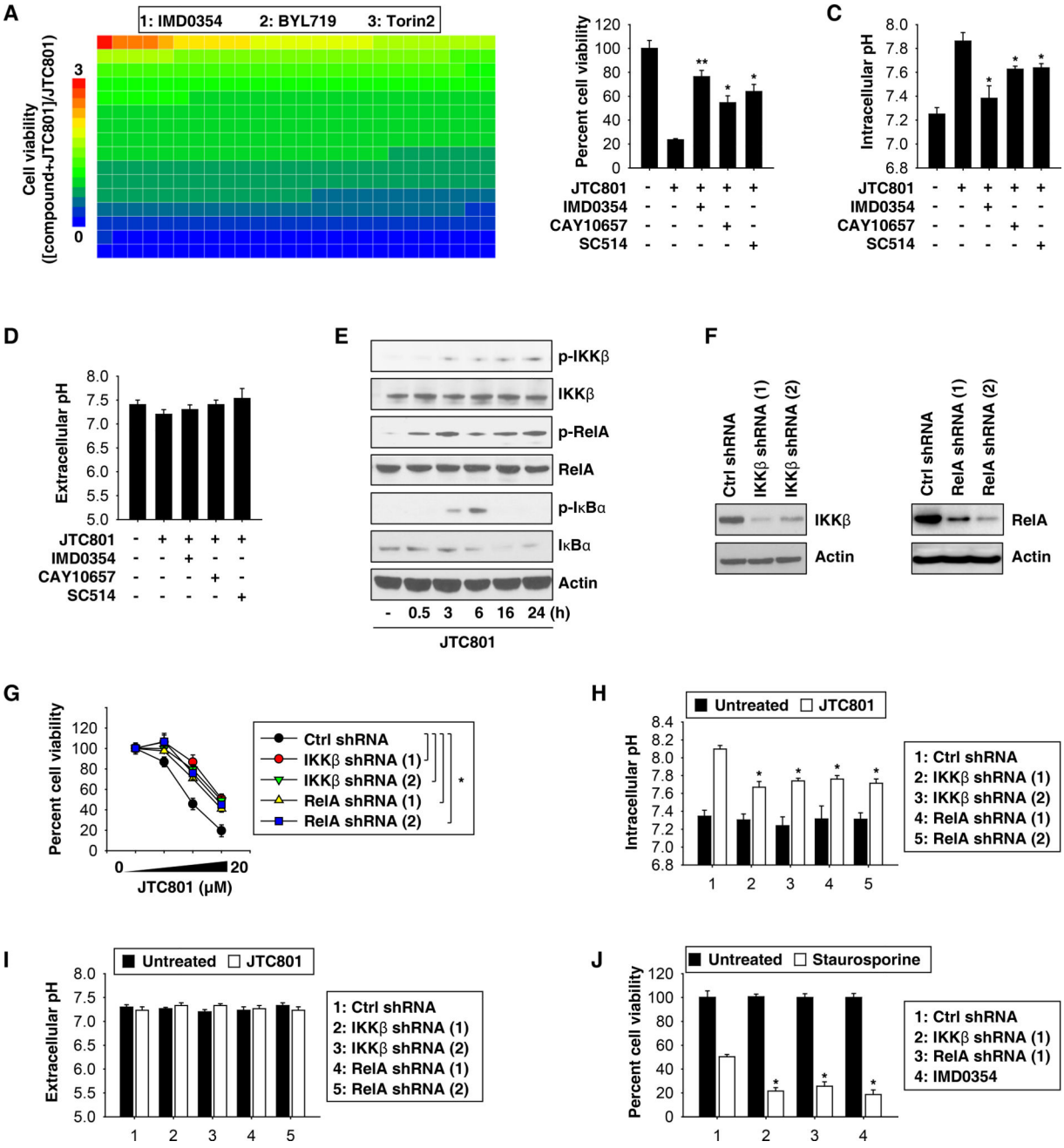


**Fig. 4. Activation of NF-κB contributes to alkaliptosis**

(A) PANC1 cells were treated with JTC801 (10 μM) in the absence or presence of an inhibitor (10 μM) for 24 hours and then cell viability was assayed. The relative effects of 416 inhibitors on anticancer activity of JTC801 are shown by the heat map. The top three inhibitors of the anticancer activity of JTC801 are listed. (B–D) PANC1 cells were treated with JTC801 (10 μM) in the absence or presence of indicated IKKβ inhibitors (10 μM) for 24 hours. Cell viability, intracellular pH, and extracellular pH were measured (n=3, *p < 0.05, **p < 0.01 versus JTC801 group). (E) Western blot analysis of expressions of indicated proteins in PANC1 cells in response to JTC801 (10 μM) for 0.5–24 hours. (F)

Western blot analysis of IKKβ and RelA expression in indicated gene-knockdown PANC1 cells. (G) Knockdown of IKKβ and RelA inhibited JTC801 (1.25–20 μM)-induced cell death at 24 hours in PANC1 cells (n=3, *p < 0.05). (H–I) Indicated gene-knockdown PANC1 cells were treated with JTC801 (10 μM) for 24 hours. Intracellular and extracellular pH was assayed (n=3, *p < 0.05 versus untreated group). (J) Indicated gene-knockdown PANC1 cells were treated with staurosporine (1 μM) with or without IMD0354 (10 μM) for 24 hours. Cell viability was measured (n=3, *p < 0.05 versus control shRNA group).

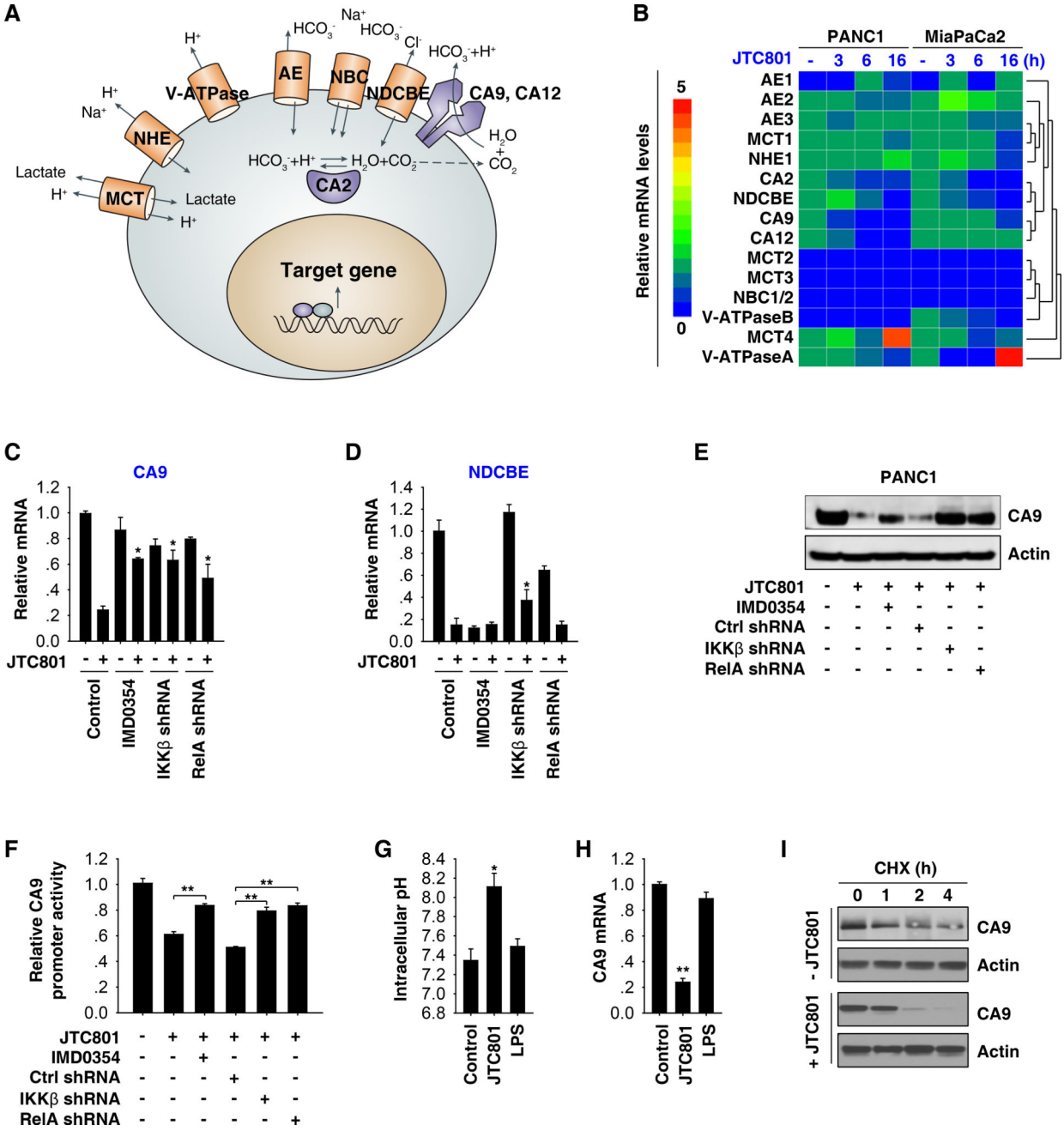


**Fig. 5. CA9 is a negative target of NF-κB in alkaliptosis**

(A) Schematic depicting proteins involved in pH regulation within a tumor cell. (B) PANC1 and MiaPaCa2 cells were treated with JTC801 (10 μM) for three to 16 hours and then the indicated genes were assayed using Q-PCR. The relative mRNA levels of indicated genes are shown by the heat map. (C–D) Q-PCR analysis of mRNA levels of CA9 and NDCBE in indicated PANC1 cells in response to JTC801 (10 μM) in the absence or presence IMD0354 (10 μM) for 24 hours (n=3, *p < 0.05 versus control JTC801 group). (E–F) In parallel, the protein expression and promoter luciferase activity of CA9 were measured (n=3, **p < 0.01). (G–H) PANC1 were treated with JTC801 (10 μM) or LPS (500 ng/ml) for 16 hours

and then intracellular pH and CA9 mRNA were assayed (n=3, *p < 0.05, **p < 0.01 versus control group). (I) PANC1 cells were treated with JTC801 (10 μM) and cycloheximide (CHX, 20 μg/ml) for indicated time points. Cell lysates were subjected to western blot analysis with anti-CA9 and anti-actin antibodies.

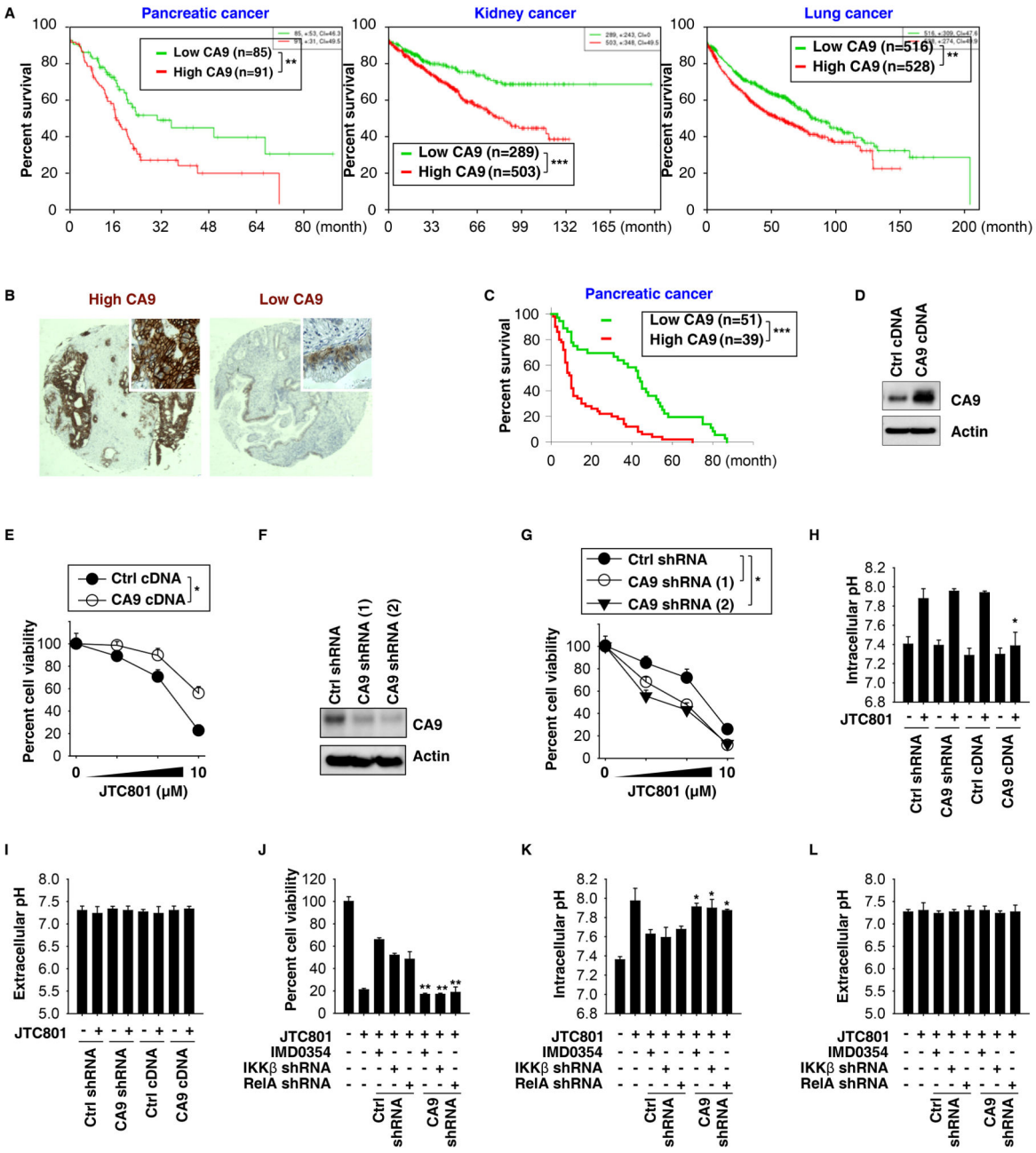


**Fig. 6. CA9 downregulation contributes to alkaliptosis**

(A) Survival analysis of patients with low or high CA9 mRNA expression levels in pancreatic, kidney, and lung cancer from the SurvExpress online gene expression database (http://bioinformatica.mty.itesm.mx:8080/Biomatec/SurvivaX.jsp; **p < 0.01, ***p < 0.001). (B, C) Higher level of CA9 expression was associated with shorter survival times of patients with pancreatic cancer. Representative tissue microarray spots stained for higher or lower CA9 expression by immunohistochemistry are shown in panel B (***p < 0.001). (D) Western blot analysis of CA9 expression in CA9-overexpression PANC1 cells. (E) Overexpression of CA9 inhibited JTC801-induced cell death at 24 hours in PANC1 cells

(n=3, *p < 0.05). (F) Western blot analysis of CA9 expression in CA9-knockdown PANC1 cells. (G) Knockdown of CA9 increased JTC801-induced cell death at 24 hours in PANC1 cells (n=3, *p < 0.05 versus control shRNA group). (H, I) Intracellular and extracellular pH was assayed in indicated PANC1 cells in response to JTC801 (10 μM) for 24 hours (n=3, *p < 0.05 versus control group). (J–L) Knockdown of CA9 restored JTC801-induced cell death in NF-κB-inhibition (IMD0354 [10 μM]) or - knockdown (IKKβ shRNA or RelA shRNA) PANC1 cells. In parallel, intracellular and extracellular pH was assayed (n=3, *p < 0.05, **p < 0.01 versus control shRNA group).

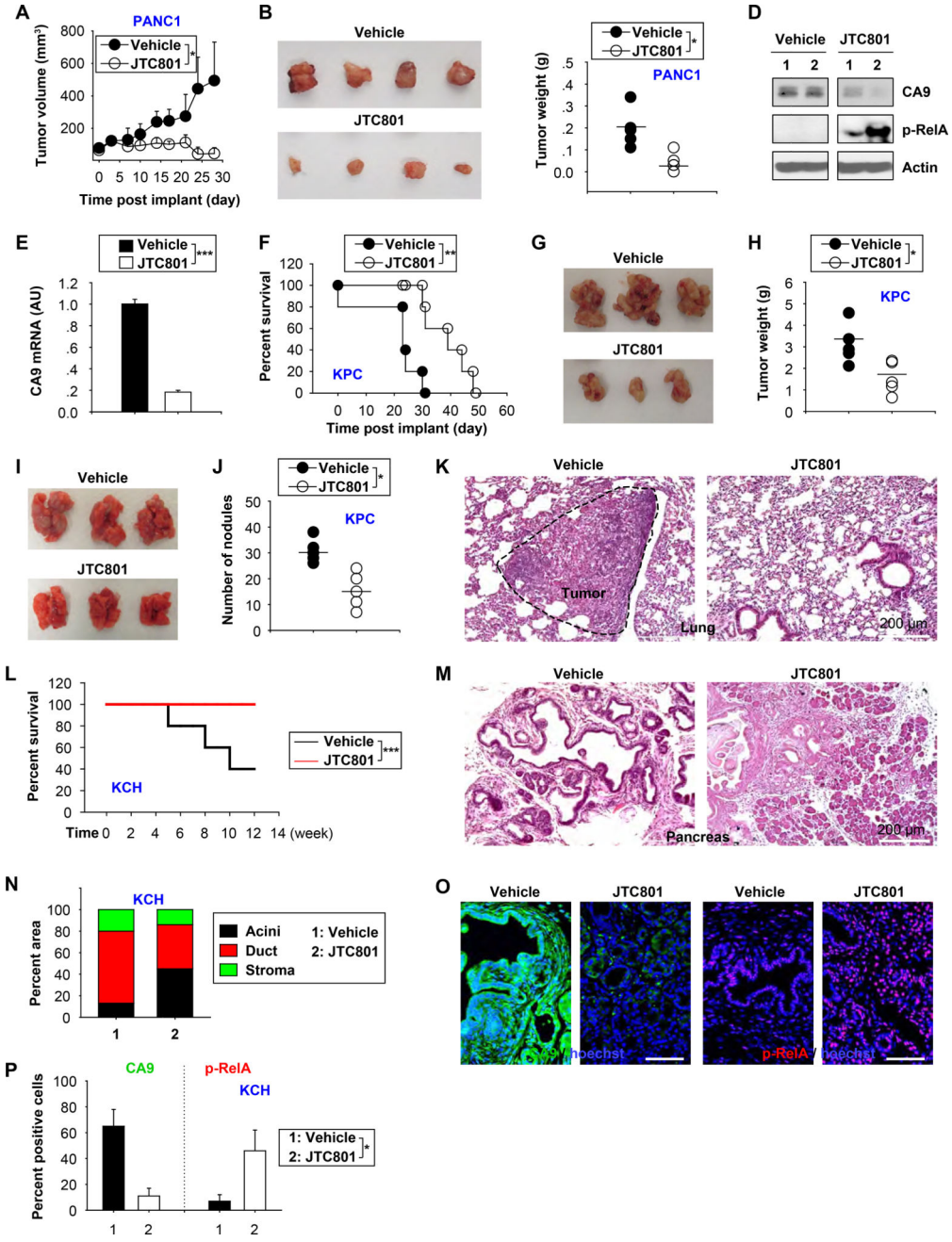


**Fig. 7. Anticancer activity of JTC801 *in vivo***

(A) Oral injection of JTC801 (20 mg/kg, once every day, at day seven for two weeks) inhibited tumor growth in a xenograft model of PANC1 tumor models (n=8 mice/group, * $p < 0.05$). (B) Representative photomicrographs of isolated tumors at day 28. (C–D) In parallel, tumor weight (C), indicated protein expression (D), and CA9 mRNA (E) were assayed at day 28 (n=5 mice/group, * $p < 0.05$, *** $p < 0.001$). (F) Oral injection of JTC801 (20 mg/kg, once every day, at day seven for three weeks) prolonged C57BL/6 mouse survival of orthotopic KPC tumor models (n=10 mice/group, ** $p < 0.01$). (G) Representative photomicrographs of isolated tumors at day 26. (H) In parallel, tumor

weights were assayed at day 26 (n=5 mice/group, * $p < 0.05$). (I) Oral injection of JTC801 (20 mg/kg, once every day, at day seven for two weeks) limited the formation of lung metastasis in C57BL/6 mice based on tail vein injection of KPC cells. (J–K) The number of tumor nodules (J) and histology (K) in lung were assayed at day 28 (n=5 mice/group, * $p < 0.05$). (L) Oral injection of JTC801 (20 mg/kg, twice per week, started at four weeks of age for four weeks) prolonged survival in KCH mice at 12 weeks of age (n=10 mice/group, *** $p < 0.001$). (M–P) In parallel, pancreatic histology (M, N) and relative expression of CA9 and p-RelA in the pancreas (O, P) were assayed (n=5 mice/group, * $p < 0.05$).